

On the working principles of Energy Saving Devices

Tom van Terwisga^{1,2}

¹Maritime Research Institute Netherlands (MARIN), Wageningen, The Netherlands

²Delft University of Technology, Faculty of 3ME, Maritime and Transport Technology, Delft, The Netherlands

ABSTRACT

The aim of this paper is to explain the principal mechanisms for the reduction in power demand by so called “Energy Saving Devices” (ESDs). This paper follows a similar approach as taken by Wald (1965) and Dyne (1995), where the authors use considerations of the momentum and energy equations.

Different energy saving concepts are evaluated on their contribution to the abatement of energy losses. The discussion on hydrodynamic mechanisms is then focused on Pre- or Upstream Ducts where four different mechanisms are hypothesized. The effect of these mechanisms is then investigated for a systematically varied series of Pre-Ducts on an axisymmetric body in deeply submerged conditions. It is concluded that the benefits of this Pre-Duct configuration do not come from the same principles as used by ducts around propellers, nor that they come from an improved propeller-hull interaction. It is recommended to further study the remaining hypothesis that a Pre-Duct conditions the flow into the propeller in a favorable way so that the propeller operates at a higher efficiency.

Keywords

Energy Saving Devices, Energy considerations, CFD

1. INTRODUCTION

This paper aims to review working mechanisms of frequently used Energy Saving Devices. Before discussing the working principles, the energy losses produced by an open propeller, and a method to assess the effect of propeller-hull interaction on delivered power is reviewed. After a review of working mechanisms, the discussion is focused on the principles of pre- or upstream ducts. Four different mechanisms are hypothesized, which are subsequently investigated by CFD computations on a systematically varied series of Pre-Ducts on an axisymmetric deeply submerged body. The paper concludes with an evaluation of these mechanisms for the Pre-Duct and draws conclusions on the computational modeling of the propeller in CFD computations.

2. ENERGY BALANCE CONSIDERATIONS

This section aims at introducing the energy loss terms in the wake of the propelled ship, which fully accounts for the power required to propel the ship.

Let us start with the relatively simple case of a deeply submerged axisymmetric hull in an axial flow as depicted in Figure 1.

An interesting property of the velocity distribution in this plane follows from Newton’s second law. The resistance force that is experienced by the hull due to the water flow, is completely represented by the change in momentum flux between the incoming, undisturbed momentum flux, and the outgoing momentum flux at the considered transverse exit plane in the wake.

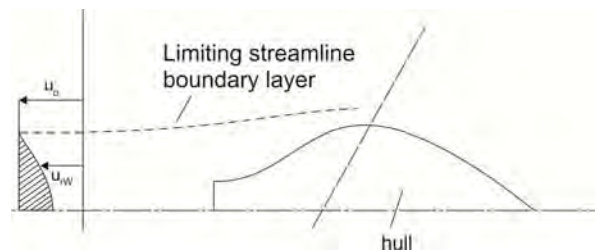


Figure 1 Velocity profile in the wake of the bare hull. The hatched area in the velocity profile indicates the hull induced velocities.

We now introduce a propeller, to counteract the resistance force on the hull (see

), and observe that the wake and the resistance of the hull have changed due to the propeller suction. We can now rewrite the momentum equation as follows (see e.g. Wald (1965)):

$$R_p - T = \rho \int_{A_{WP}} u_x (u_x - U_0) dA \quad (1)$$

Where R_p = resistance force on the hull with active propeller and subscript P refers to the self propelled condition.

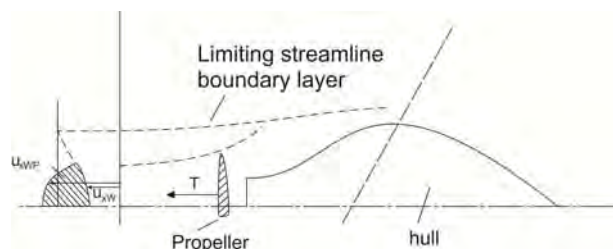


Figure 2 Velocity profile in the wake of the self propelled hull. The hatched area in the velocity profile indicates the propeller induced velocities.

For a steady state condition, the thrust force should balance the resistance force R_p of the hull, implying that the right hand side of (1) equals zero. Please note that the resistance of the hull in the self propelled condition is likely to be different from the resistance of the bare hull, the difference being accounted for by a thrust deduction fraction t :

$$T(1-t) = R_{bh} \quad (2)$$

An important conclusion from Newton's second law and the momentum balance consideration is that whatever ESD we mount to the hull, it does not produce a net change in momentum flux between in and outflow plane, as long as the ship moves at a steady speed. This implies that a change in propeller thrust, cannot directly be interpreted as a gain or loss in power requirement. Consequently, all effects of ESDs must appear through an effect in the energy losses in the flow.

These energy losses are obtained from a consideration of the energy balance of a control volume that contains the ship-propulsor system. This energy balance in words states that the power needed to propel the ship must be equal to the hydraulic losses that can be traced back in the wake of the ship. The energy balance for the self propelled ship in steady state, can thus be written as:

$$P_D = AXL_{WP} + PRESL_{WP} + TRANS�_{WP} \quad (3)$$

The three loss terms on the right hand side can be expressed in local velocities and pressures by applying the conservation laws to a control surface in a fluid. An additional term is present in the pressure loss term, that should be expressed in terms of heat. This energy flux results from a conversion of kinetic energy into heat caused by viscous dissipation.

Let us now take a closer look at the different loss terms. The rationale for this analysis is that if we know the magnitude and the origin of the energy loss, we may be able to recover part of these energy losses with an Energy Saving Device.



Figure 3 defines the different (time averaged) axial velocity profiles that can be distinguished in the wake of the ship and the constituting components.

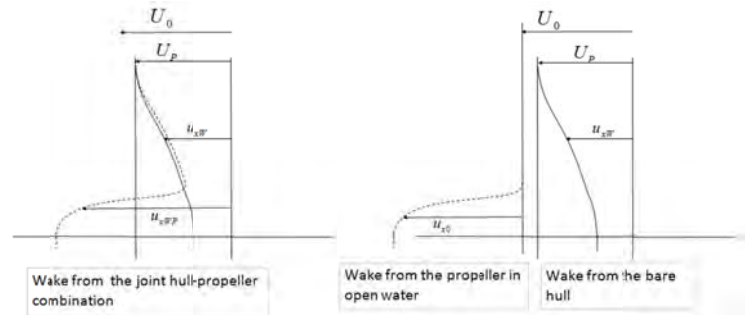


Figure 3 Axial velocity profiles in the wake of the ship, the propeller and the hull

2.1.1 Axial energy losses

The axial losses for a deeply submerged and self-propelled axisymmetric body consist of the retarded flow by the hull resistance, and of the accelerated flow by the propulsor.

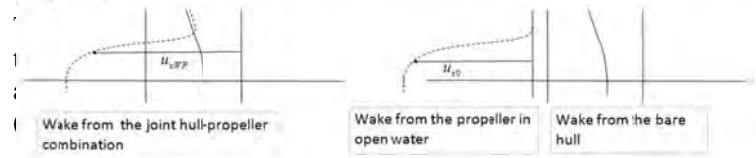


Figure 3). For a given thrust, the required axial acceleration of the flow follows from the momentum equation and from that, the axial component of the energy flux.

The term "axial losses" is also used in the actuator disk model for a propeller, where the propeller is represented by a disk in a non-viscous flow, which exerts an axial force on the flow. This model yields the following relation for the axial losses in the far field :

$$AXL_i = \iint_{A_f} \frac{1}{2} \rho \left[(u_{x0}^2 - U_0^2) \right] u_{x0} dA \quad (4)$$

These propeller axial losses are accounted for by the well known ideal efficiency η_i , which solely depends on the propeller loading C_T :

$$\eta_i = \frac{TU_0}{AXL_i} = \frac{2}{1 + \sqrt{1 + C_T}} \quad (5)$$

Where AXL_i refers to the axial losses in the actuator disk model

$$C_T = \frac{T}{\frac{1}{2} \rho U_0^2 A_p}$$

and A_p = propeller disk area.

For a real propeller in open water conditions, the non-uniform velocity distribution and viscous losses contribute to additional axial losses.

Axial losses cannot easily be separated in a real flow as the origin of the change in axial velocity cannot be traced. These combined losses in the propeller-hull system will be referred to as axial losses AXL_{WP} in the following, where the subscript WP refers to the Wake of the self Propelled condition.

The non-uniform velocity distribution does have an effect on the axial losses, as was demonstrated for the wake of a waterjet by Scherer et al. [2001]. The effect of the non-uniformity of this wake was computed to give 2 to 3% more axial kinetic energy losses than a uniform outflow would give at the same thrust coefficient.

2.1.2 Pressure losses

The pressure losses and the viscous dissipation term, will be referred to as Pressure Losses in the following:

$$PRESL_{WP} = \iint_{A_{WP}} (p - p_0) u_{xWP} dA + \psi_{dissWP} \quad (6)$$

2.1.3 Transverse losses

Together with the axial losses, there is an outflux of transverse kinetic energy in the wake. These so called transverse losses consist to a large extent of rotational losses for a propeller in open water conditions. In self propelled condition, the transverse velocities are likely to increase due to the slope of the buttocks and waterlines in the aftbody of the hull. The transverse losses are defined by the energy flux containing the tangential and radial velocity components:

$$TRANSL_{WP} = \iint_{A_{WP}} \frac{1}{2} \rho [u_{r0}^2 + u_{\phi 0}^2] u_{x0} dA \quad (7)$$

Analogous to the axial losses, the non-uniformity in the wake also causes an increase in transverse energy losses. This is caused by the finite number of blades and the radial load distribution over the blades of a propeller in open water. In addition, a non-uniform inflow field from the hull causes a variation in radial loading distribution over the propeller blade, thereby causing extra transverse energy losses.

3. ASSESSMENT OF ENERGY LOSSES

3.1 Propeller Open Water Analysis

To get an appreciation of the magnitude of the energy losses by a propeller, we will consider the propeller open water case here. An extensive study on the energy losses typical for a propeller in open water has been published by Olsen [2004].

To find the relation with the energy losses, the open water efficiency η_0 can be written as:

$$\eta_0 = 1 - \frac{AXL_0}{P_D} - \frac{VISCL_0}{P_D} - \frac{ROTL_0}{P_D} \quad (8)$$

It is noted that the sum of the pressure losses and transverse losses, as identified in the preceding section, have been replaced by the sum of loss terms that refer to the origin of the loss, i.e. viscosity and rotation. The reason is that this classification better links up with existing literature and with the often non-viscous potential flow codes for propeller analysis.

The axial loss term can be approximated by the ideal efficiency:

$$\eta_i \approx 1 - \frac{AXL_0}{P_D} \quad (9)$$

It should be noted here that the ideal efficiency accounts for axial kinetic energy losses in the non-viscous flow in which an actuator disk represents the propeller. This actuator disk consists of a thin disk with a uniform load distribution, causing a sudden pressure jump in the flow. This model does consequently not account for the finite number of blades nor does it account for the radial loading distribution, which does cause additional losses (see e.g. Olsen [2004]).

An estimate of the different propeller losses is presented in Figure 4. This graph shows a comparison between the ideal efficiency and the open water efficiencies of a representative four bladed B series propeller with a blade area ratio $A_E/A_0=0.70$ for three different pitch settings. The operating range of interest is indicated with representative thrust loading values for a containership, an LNG carrier and a tanker.

Figure 4 shows that a major part of the losses is caused by axial kinetic energy losses AXL_0 (approx. 16 to 26 % point), the highest thrust loading C_T producing the highest axial losses. The sum of the rotational and viscous losses ranges from approx. 17-19% point. The ratio of these losses can be affected by the choice of propeller rotation rate and propeller pitch. For a given thrust requirement, a higher pitch angle will reduce the rotation speed and will thus reduce the viscous losses at the cost of higher rotational losses.

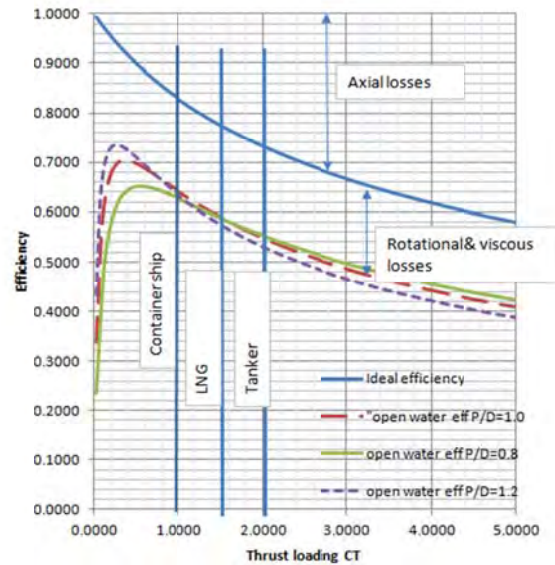


Figure 4 Relative energy loss terms for B-series propeller P/D=1.0

3.2 Propeller-hull interaction

A classical treatment of the energy losses in the propeller-hull interaction problem is given by Wald [1965]. Wald derives relations for the thrust deduction and ideal efficiency of an actuator disk that is used as a model in which both potential flow as well as viscous wake effects are important. Wald thereby limits his considerations to the effect of propeller-hull interaction on the axial energy losses AXL_{WP} .

It is found that the thrust deduction fraction t tends to decrease when the propeller is located in a region of retardation of the flow due to *viscous* effects, but tends to increase when the wake retardation is due to *potential* flow effects. The efficiency is influenced in opposite directions by these conditions.

Wald derives an expression for the ideal efficiency including the effect of thrust deduction and wake, which can be written in the following form:

$$\eta_{i\text{behind}} = \frac{2}{1 - w_v + \sqrt{(1 + C_T)}} \quad (10)$$

Where w_v = viscous component of the wake, which can be obtained from the difference in total pressures in the propeller plane (without active propeller), from:

$$\frac{1}{2} \rho U_0^2 (1 - w_v) + p_0 = \frac{1}{2} \rho u_1^2 + p_1 \quad (11)$$

Where subscript 1 refers to the propeller plane when the propeller is absent, corresponding to the nominal viscous component of the wake.

In the case of a ducted propeller, a similar relation is obtained for the ideal efficiency (actuator disk in a free stream) by e.g. Oosterveld (1970):

$$\eta_i = \frac{2}{1 + \sqrt{1 + \tau C_T}} \quad (12)$$

Where $\tau = T_p/T_T$ the ratio between propeller thrust and total thrust.

This ratio deviates from unity in the case of a propeller duct for example, but can also be used to express the effect of a thrust deduction fraction on efficiency, thereby assuming a uniform flow through the disk. In the case of an accelerating duct, the thrust ratio τ is smaller than unity and an increase in ideal efficiency occurs. This thrust ratio has a unique relation with the mean velocity through the propeller disk (Oosterveld 1970):

$$\frac{u_p}{U_0} = \frac{1}{2\tau} \left(1 + \sqrt{(1 + \tau C_T)} \right) \quad (13)$$

When we now know the change in mass flow through the propeller disk, due to e.g. a propeller duct or a Pre-Duct, we can in principle compute the thrust ratio τ (equivalent to the change in thrust deduction factor $(1-t)$), which then gives us the change in ideal efficiency. This procedure is based on the assumption that the change of the effective viscous wake fraction w_v with propeller suction, is similar to the change in nominal wake (without propeller). This assumption is likely to be limited to the lighter thrust loadings only (say $C_T < 1$).

The effect of a duct resulting in a change in mass flux through the propeller disk, as well as by a change of the viscous wake fraction, can now be estimated from eq. (10) once detailed data on velocities and pressures are available from CFD. This will be demonstrated in the worked example on Pre-Ducts.

4. WORKING PRINCIPLES OF ESDs

The previous chapter has classified the energy losses that occur in the wake of a self propelled ship. With this knowledge, we attempt to better understand the working mechanisms of three different types of ESDs.

To this end, it is convenient to study the effect of ESDs on a simple body (e.g. axisymmetric) in deeply submerged condition (no free surface) in a potential flow. And from thereon, gradually add complexity, so as to make a step towards a more 3D ship afterbody in a double body flow (still no free surface), to then add viscosity and finally add the free surface. Although it is realized that ESDs might affect the wavemaking drag, this effect is considered of secondary importance and will subsequently be neglected in the following.

The following considerations deal with a 3D ship in a double body, potential flow, unless indicated otherwise.

It is interesting to see what is happening in a potential flow when we mount a fin to the aftbody, e.g. to improve the flow into the propulsor. Although a non-lifting body would have a zero contribution to the resistance, a finite fin does contribute to the drag through the shed trailing vortex system, causing the total force vector to act with a component in the downstream x-direction because of the shed vortex system. The strength of the shed vortices in a potential flow follow from application of the Kutta Condition at the Trailing Edge of the fin or foil. This vortex system occurs in the downstream outlet plane as tangential velocities that represent transverse momentum, which is at the cost of the axial momentum for equal power input. The resulting velocity deficit in x-direction is associated with the induced drag of the foil. Only in the case of an infinite 2D foil or a circular foil with equal loading distribution, no vortices will be shed and the foil system may deliver an internal load in x-direction. However, it still will not deliver a positive contribution to thrust.

A passive foil system (fixed to the hull) might however produce a net thrust to the system, if this foil system is placed in the propeller induced velocity field.

4.1 Pre-Ducts

Before considering Pre-Ducts or upstream mounted ducts, let us first consider the duct of a ducted propeller. The reason that a nozzle or duct around a propeller is contributing positively to the overall efficiency is because it accelerates the flow through the propeller plane (pump action), thereby increasing the mass flux through the propeller (eq. (13)) which gives rise to a higher ideal efficiency (equivalent to lower axial kinetic energy losses eq. (10)). For this purpose, the nozzle is best mounted as close to the propeller as possible, since the actuator induced velocities will disappear gradually with downstream and upstream distance to the actuator.

We thus conclude that the duct from a ducted propeller effectively reduces the axial kinetic energy losses. Furthermore, by increasing the flow rate through the propeller disk, it may also increase the capture of viscous

wake through the propeller disk, thereby increasing the propeller-hull interaction contribution to the efficiency, according to Wald [1965]. The net contribution to efficiency of this viscous wake effect depends on the fraction of the viscous wake through the propeller disk.

These two efficiency enhancing mechanisms (increase of flow rate and viscous wake fraction) can also be assigned to Pre-Ducts. It should be noted here however, that due to the reduction of actuator induced velocities with distance from the actuator, the upstream duct must necessarily be less efficient in a potential flow than a duct mounted in the propeller (actuator) plane.

Based on the above considerations and experience in analyzing Pre-Ducts, the following working mechanisms are hypothesized for a Pre-Duct:

1. Increasing the mass flow through the propeller, resulting in lower axial losses by the propeller. This is also the a main principle of a ducted propeller.
2. Use of propeller hull interaction to reduce axial losses (through increase of the viscous wake fraction wv) or decrease of thrust deduction t .
3. To increase uniformity of the far wake by reducing effects of non-uniformity through:
 - a. Changing the radial thrust distribution of the propeller. If more thrust is generated at lower radii, this could result in a reduction of the torque and with that of the efficiency. It must be noted that the radial thrust distribution can also be altered by changing the radial pitch distribution of a propeller. If this gives a positive effect, the radial distribution of the propeller is probably not optimal.
 - b. Changing the circumferential velocity distribution into the propeller. If the propeller inflow is more uniform, it is expected that the thrust distribution will also be more uniform. This could lead to a more uniform slipstream and with that less kinetic losses in the slipstream.
 - c. Non-uniformity effects of propeller thrust distribution on thrust deduction. If the propeller loading is higher close to the hull, this is likely to increase thrust deduction.
 - d. The duct can re-direct the flow in axial direction to the propeller. This will have a positive effect on a more evenly distributed blade loading in circumferential direction, which will give the same benefits as mentioned under the three previous effects
4. In case of extensive flow separation on the aft ship, the Pre-Duct could lead to a decrease of the extent of the separated flow over the aft ship. This would result in a reduction of the viscous pressure resistance, which would appear in a reduced thrust deduction.

The case of a Pre-Duct on an axisymmetric body is worked out in the following section.

4.2 Pre- and post swirl stators

As discussed in the introduction to this section, passive fin systems can never improve the overall efficiency of the propulsor-ship system by creating thrust. It possibly could alleviate the resistance, particularly by interfering favourably with the Free Surface. When looking at the energy losses that are created by the propulsor-hull system, we can however distinguish rotational losses that could be recovered, either by a secondary rotating propeller like system (e.g. in the case of contra rotating propellers, a Grim's vane wheel or a PBCF), or by static stators either mounted upstream or downstream of the propeller. These devices are then to decrease the rotational kinetic energy losses at the benefit of increasing the axial kinetic energy and momentum flux, and thus thrust.

When mounting a pre- or post swirl stator, a redistribution of torque between stator and propeller occurs in such a way that the propeller blades are more heavily and uniformly loaded, resulting in a reduction of rotation rate of the propeller at equal thrust. This in turn, also reduces the viscous losses incurred by the propeller.

4.3 Rudder bulbs

The effect of a rudder bulb has been studied in detail by doing a large number of CFD computations, using different computational models to represent the propeller. Amongst the different models, actuator disks with and without swirl production were used, as well as a RANS-BEM coupling, where the propeller was modeled through a BEM method. The results of this study indicate that the benefit of a rudder bulb can both be attributed to a smaller thrust requirement, as well as to a relatively lower torque demand.

4.4 Combined systems

If Energy Saving structures are going to be fitted, it makes sense to investigate whether or not multiple energy loss reductions can be achieved. And although there is often a coupling between the four different types of energy losses (axial kinetic, transverse (often largely rotational) kinetic, viscous and non-uniformity losses), it is to be investigated whether this coupling is sufficiently weak to successfully abate losses simultaneously.

Successful examples of combined systems are Contra Rotating propellers (primarily rotational losses, but also viscous losses and axial losses), Mewis duct (axial, rotational and non-uniformity losses), as well the Grim's Vane Wheel (axial, rotational).

5. NUMERICAL ANALYSIS OF A PRE-DUCT

5.1 Set-up of systematic Pre-Duct series

To verify, or better falsify, the hypotheses on the working mechanisms of a Pre-Duct, this sections summarizes some of the results of CFD computations with the MARIN RANS solver REFRESCO on the powering performance of a systematically varied Pre-Duct series, mounted on an axisymmetric body. Pre-Ducts are chosen here because their energy saving mechanisms are not free of debate.

The rationale behind the choice for an axisymmetric body has a number of reasons. First, it yields an axisymmetric flow into the propeller, avoiding the effects of any circumferential velocity gradients. Secondly, it is computationally efficient. And thirdly, it allows for the energy considerations as used by Wald (1965).

A systematic series of Pre-Ducts is designed, keeping both the profile geometry and the leading edge position the same. The loading on the Pre-Duct is increased by moving the trailing edge outward (from Duct D1), with one additional duct D7, having the lightest loading.

The computational domain consists of two large cylinders, joined together by means of a non-conformal interface, where the cell boundaries at the interface do not match. This gives the advantage that only the grid containing the Pre-Duct needs to be changed, where the propeller grid remains the same.

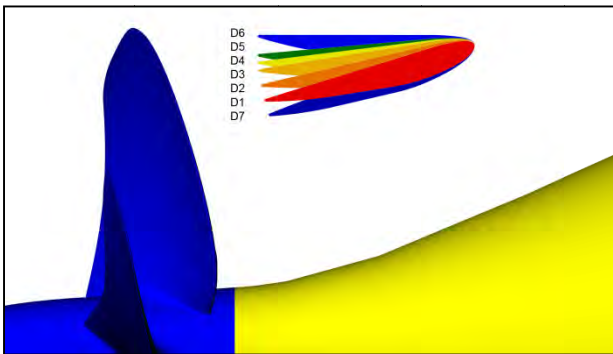


Figure 5 Systematic variation series A

Table 1

	# Elements	# Surface Elements	Max y^+	Average y^+
GRID1 Torpedo	12.3M	-	-	-
Axi-symmetric body	-	0.8M	1.0	0.62
Pre-Duct	-	0.1M	2.2	0.7
GRID2 Propeller	25.6M	-	-	-
Propeller	-	1.1M	2.1	0.3
Hub	-	0.1M	0.3	0.1

The iterative convergence of the velocities are below 10^{-3} in the L_∞ norm (max residual in whole computational domain) and well below 10^{-5} in the L_2 norm (RMS value of all residuals). For the pressure and turbulence quantities the iterative convergence is often to be seen below 10^{-4} or lower in the L_∞ norm. Further convergence is possible, but would not lead to other resulting forces or conclusions.

5.2 Results of Pre-Duct computations

The performance of the different Pre-Duct geometries is presented in Figure 6, where the thrust and torque of the

propeller with the various Pre-Ducts from Figure 5 are plotted relative to the performance of the open propeller. Most of the computations were conducted for a thrust loading $C_{Ta} = 1.60$. The performance for two ducts has been computed for a higher propeller thrust loading of $C_{Ta} = 2.42$, which is an increase in thrust loading of some 50%. The thus obtained thrust loadings are considered representative for a large number of full block ships (see e.g. Meuwis [2011]). The thrust loading C_{Ta} used here is based on the advance velocity:

$$C_{Ta} = \frac{T}{\frac{1}{2} \rho U_0^2 (1 - w_v)^2 A_p} \quad (14)$$

The results for the increased thrust loading on the Ducts 3 and 4 are indicated in Figure 6 as well, the arrows indicating increasing thrust loading.

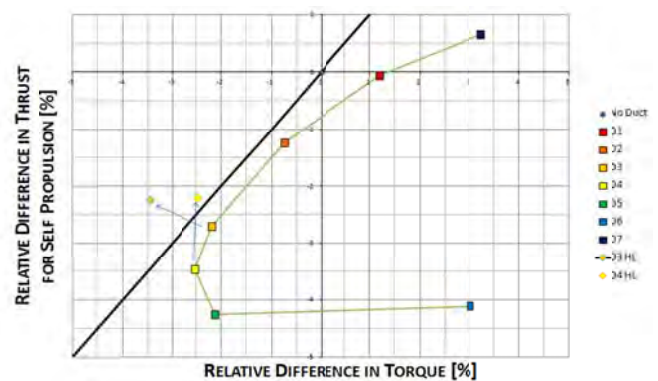


Figure 6 Performance plot for the systematic variation series A

During these computations, the propeller rotation rate was kept at a constant rpm, and hence the propeller did not operate at the self-propulsion point ship, as both the thrust demand and the wake of the ship is changed slightly for every other Pre-Duct. The required power for the new configuration is then obtained from:

$$P_D = 2\pi Qn \quad (15)$$

To account for this deviation in rotation rate from the self-propulsion point rotation rate, it has been assumed (and numerically verified) that the Thrust-Torque relation in terms of dT/dQ is unaffected. The required power for any Pre-Duct configuration can thus be assessed from the computed Thrust-Torque relation and a correction in torque for the self-propulsion point. The correction in torque is thus obtained from the horizontal distance between a calculated point and the $\Delta T = \Delta Q$ line. A further correction is then required for the propeller rotation rate, deviating slightly from the rotation rate at this self-propulsion point. A first estimate of this correction can be made by assuming that both the thrust and the torque coefficient remain constant for a small increase or decrease of the propeller rotation rate. This is strictly speaking not true, but corrections are small and will only amplify the thus obtained power difference with increasing rotation rate correction.

The results from this Power correction procedure are plotted in Figure 7 as the ratio of required power P_D between the duct configuration and the open propeller.

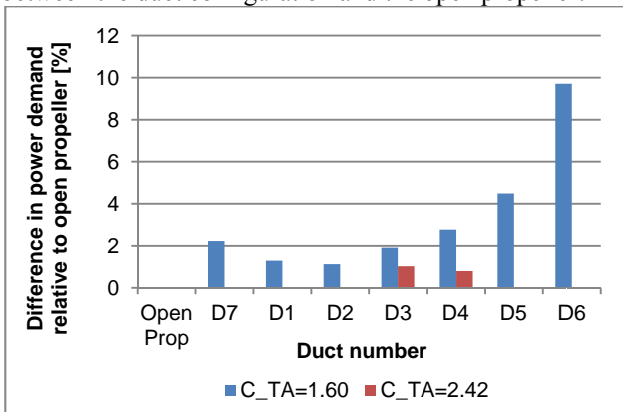


Figure 7 Ratio of required power P_D to the power required for the same open propeller for the various duct geometries

One can observe that for all Pre-Duct cases, the power required for a given speed is higher than for the reference case with open propeller. The best performing duct for the lower C_{Ta} is approx. 1% worse in required power than the reference case without duct. The increased propeller loading has a positive effect on the duct effectiveness, but the best duct (D3 HL) still requires some 1% increase in power demand relative to the reference open propeller.

This finding is somewhat contradictory to many results that were obtained from model tests, where savings up to 7% have been claimed for full block ships (e.g. Hollenbach SMP'11). In many of these cases any large scale boundary layer flow separation could not be detected, suggesting that at least in some cases, the avoidance of large scale separation (mechanism 4 of Section 4.1) could not be confirmed.

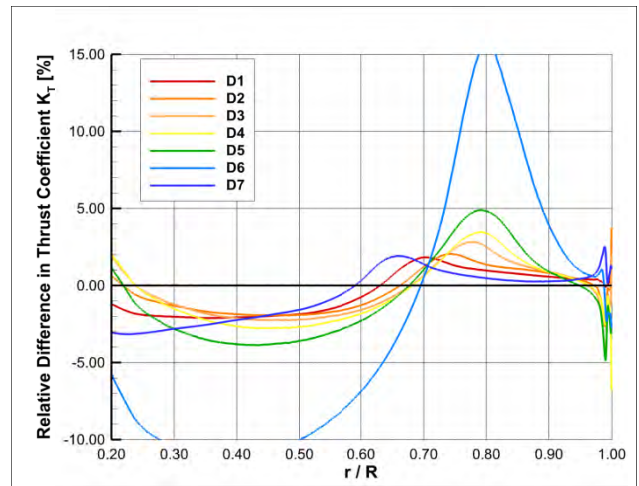
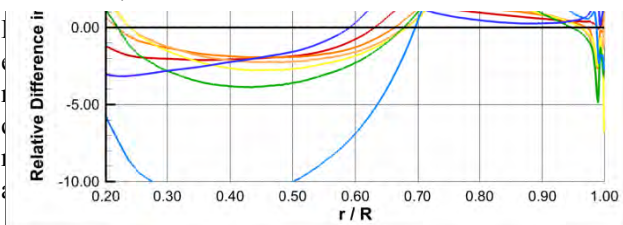


Figure 8 Relative radial thrust distribution for the seven different Pre-Ducts

The hypothesized mechanisms 3c and 3d cannot be evaluated because of the axisymmetric flow in this case.

Let us now take a closer look at the mechanism similar to that of the propeller duct, where the propeller is unloaded by the duct, such that the axial losses of the propeller are diminished. In this case, the mean velocity through the propeller disc should be increased. The effect of this pumping power by the Pre-Duct (or thrust unloading) can be assessed by the relations (12) and (13) when the thrust loading of the parent propeller is known and the mass flux through the propeller disk is evaluated from the CFD results. It can be observed from the change in massflow in Figure 9 that the mean velocity through the propeller disk increases up to some 4% (up to 6% after correction for the self propulsion point).

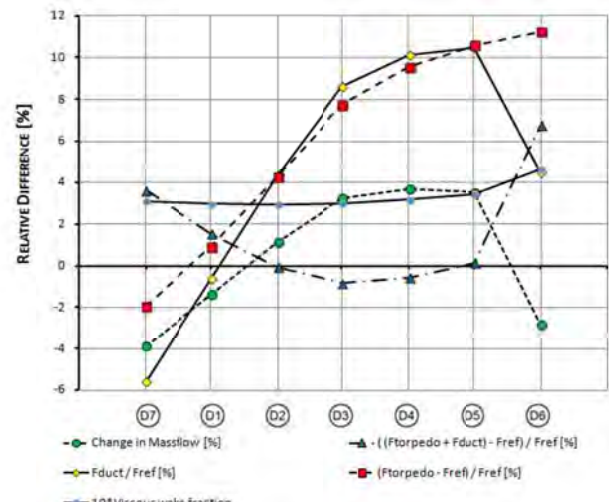


Figure 9 The relative changes in mass flow, forces and viscous wake

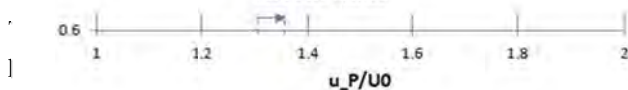


Figure 10 and appears to give a propeller unloading of some 5% for a $C_{Ta}=1.60$. The effect on the ideal efficiency in behind condition follows from eq. (12) and appears to result in an increase of less than 1% for the

duct with the highest flow acceleration D4. The ducts D2 and D3 give the best performance from a powering perspective however.

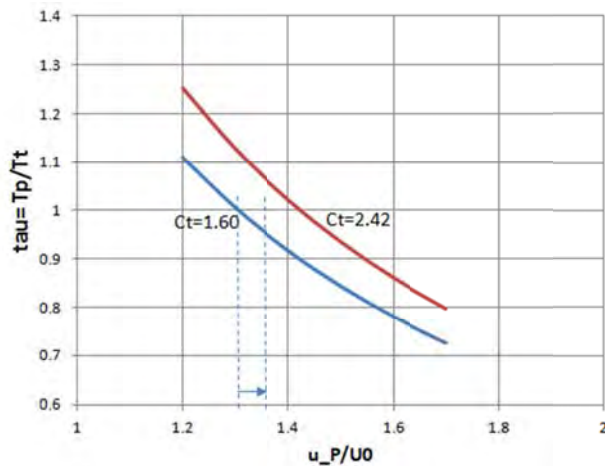


Figure 10 Relation between mean velocity through propeller disk u_p/U_0 and propeller thrust ratio τ

The effect of duct geometry on viscous wake is also shown in Figure 9. The ducts D1-D3 show an almost constant viscous wake fraction of 0.29-0.30, where no separation on the ducts has occurred. For the highest loaded ducts, separation occurs on the duct itself, causing the increasing viscous wake fraction. This effect cannot give a net positive contribution to the efficiency.

The above results lead to the conclusion that the Pre-Ducts do not contribute in a similar way to a higher efficiency as ducts around a propeller (see e.g. Oosterveld (1970)). Also their effect on improving the propeller hull interaction through a possible increase in viscous wake did not lead to significant gains for a representative thrust loading of $C_{Ta} = 1.60$, based on ship speed.

This leads to the conclusion that if Pre-Ducts are successful, it must apparently be caused to a large extent by an improved propeller efficiency due to a change in the 3D velocity field. This remaining hypothesis can not be evaluated on this axi-symmetric body and is yet to be verified.

On the modeling of the propeller for this type of computations, it is concluded that the effect of a non-uniform inflow and/or inclined inflow is to be accurately represented by the method. This leaves some doubt with the typical propeller modeling in BEM codes, as they might not sufficiently accurately model this effect. RANS codes should capture this effect in theory.

6. CONCLUSIONS AND RECOMMENDATIONS

The paper starts with a review of energy losses produced by the propeller-hull system, as any Energy Saving Device needs to improve on at least one of these losses. The losses produced by a representative B-series propeller and a method to assess the effect of hull-propeller interaction are then discussed. Perhaps one of the less well understood Energy Saving Devices is the Pre- or Upstream Duct.

A CFD analysis on a systematically varied set of Pre-Ducts on an axi-symmetric body, reveals that for the thrust loading coefficient of a container vessel, no substantial benefits could be obtained, despite the fact that power reductions up to 7% have been claimed in literature for full block ships. These conclusions were typically based on model tests. It is concluded that if such benefits would occur, they must be caused by a favourable conditioning of the flow by the Pre-Duct, so that the propeller can operate at a higher efficiency. The Pre-Ducts used in this study were not able to reduce the overall power demand.

It is recommended therefore, that for a reliable assessment of the consequences in power demand, an accurate propeller modeling is necessary. This leaves doubts with the adequacy of BEM methods for such modeling, as the generally used wake modeling in these methods is not likely to accurately account for an inclined flow or strong velocity gradients. Full RANS methods are expected to offer this resolution in modeling.

7. ACKNOWLEDGEMENTS

The author is much indebted to Bart Schuiling, who performed the computations and performed the post processing with endless energy. Also the various discussions with my colleagues Arjan Lampe, Jan Holtrop, Jie Dang, Martin Hoekstra and many other colleagues are gratefully acknowledged.

The 7FP EU project GRIP is acknowledged for funding much of the research work that contributed to this paper.

REFERENCES

- Dyne, G. (1995). 'The principles of propulsion optimization'. *Trans. RINA 137*, London, United Kingdom.
- Hollenbach, U. and Reinholz, O. (2011). 'Hydrodynamic trends in optimizing propulsion'. *Second International Symposium on Marine Propulsors SMP'11*, Hamburg, Germany.
- Mewis, F. and Guiard, T. (2011). 'Mewis Duct – New Developments, Solutions and Conclusions'. *Second International Symposium on Marine Propulsors SMP'11*, Hamburg, Germany.
- Olsen, A.S. (2004). 'Energy coefficients for a propeller series', *Ocean Engineering 31*, 2004, pp401-416.
- Oosterveld, M.W.C. (1970). 'Wake adapted ducted propellers'. *PhD thesis, Delft University, Delft, The Netherlands*.
- Scherer, O., Mutnick, I. and Lanni, F. (2001). 'Procedure for conducting a towing tank test of a waterjet propelled craft using Laser Doppler Velocimetry to determine the momentum and energy flux'. *26th American Towing Tank Conference, Webb Institute*.
- Wald, Q. (1965). 'Performance of a propeller in a wake and the interaction of propeller and hull', *Journal of Ship Research*.

